



EUROfusion

WPJET1-PR(18) 21482

G Telesca et al.

**COREDIV numerical simulation of high
neutron rate JET-ILW DD pulses in view
of extension to JET- ILW DT experiments**

Preprint of Paper to be submitted for publication in
Nuclear Fusion



This work has been carried out within the framework of the EUROfusion Consortium and has received funding from the Euratom research and training programme 2014-2018 under grant agreement No 633053. The views and opinions expressed herein do not necessarily reflect those of the European Commission.

This document is intended for publication in the open literature. It is made available on the clear understanding that it may not be further circulated and extracts or references may not be published prior to publication of the original when applicable, or without the consent of the Publications Officer, EUROfusion Programme Management Unit, Culham Science Centre, Abingdon, Oxon, OX14 3DB, UK or e-mail Publications.Officer@euro-fusion.org

Enquiries about Copyright and reproduction should be addressed to the Publications Officer, EUROfusion Programme Management Unit, Culham Science Centre, Abingdon, Oxon, OX14 3DB, UK or e-mail Publications.Officer@euro-fusion.org

The contents of this preprint and all other EUROfusion Preprints, Reports and Conference Papers are available to view online free at <http://www.euro-fusionscipub.org>. This site has full search facilities and e-mail alert options. In the JET specific papers the diagrams contained within the PDFs on this site are hyperlinked

COREDIV numerical simulation of high neutron rate **JET-ILW** DD pulses in view of extension to **JET-ILW** DT experiments

G. Telesca¹, I. Ivanova-Stanik¹, R. Zagórski¹, S. Brezinsek², P. J. Carvalho³, A. Czarnecka¹, C. Giroud⁴, A. Huber², E. Lerche⁵, S. Wiesen² and JET contributors*

EUROfusion Consortium, JET, Culham Science Centre, Abingdon, OX14 3DB, UK

¹Institute of Plasma Physics and Laser Microfusion, Warsaw, Poland

²Institut fuer Energie-und Klimaforschung-Plasmaphysik Forschungszentrum Juelich GmbH, Juelich, Germany

³Instituto de Plasmas e Fusão Nuclear, Instituto Superior Técnico, Universidade de Lisboa, Lisboa, Portugal

⁴Culham Centre for Fusion Energy, Culham Science Centre, Culham, UK

⁵LPP-ERM/KMS, Association EUROFUSION-Belgian State, TEC partner, Brussels, Belgium

Email: giuseppe.telesca@ifpilm.pl

1

Abstract

Two high performance **JET-ILW** pulses, pertaining to the 2016 experimental campaign, have been numerically simulated with the self-consistent code COREDIV with the aim of predicting the power load to the target when extrapolated to DT plasmas. The input power of about 33 MW as well as the total radiated power and the average density are similar in the two pulses, but for one of them the density is provided by combined low gas puff and pellet injection, characterized by low SOL density, for the other one by gas fuelling only, at higher SOL density. Considering the magnetic configuration of these pulses and the presence of a significant amount of Ni (not included in the version of the code used for these simulations), a number of assumptions are made in order to reproduce numerically the main core and SOL experimental data. The extrapolation to DT plasmas at the original input power of 33 MW, and taking into account only the thermal component of the alpha-power, doesn't show any significant difference regarding the power to the target with respect to the DD case. **In contrast, the simulations at auxiliary power = 40 MW, both at the original $I_p = 3$ MA and at $I_p = 4$ MA,** show that the power to the target for both pulses is possibly too high to be sustained for about 5 s by strike-point sweeping alone without any control by Ne seeding. Even though the target power load may decrease to about 13-15 MW with substantial Ne seeding for both pulses, as from numerical predictions, there are indications suggesting that the control of the power load may be more critical for the pulse with pellet injection, due to the reduced SOL radiation.

Keywords: Tokamak, integrated modeling, neon seeding, JET-ILW

*See the author list of X. Litaudon et al 2017 Nucl. Fusion 57 102001

1 INTRODUCTION

In the frame of the JET contribution to establishing a consistent scenario for deuterium-tritium ITER operation, DT experiments are planned at JET for the near future. The DT JET-ILW experiments will have to be based on well developed high power-high performance DD pulses, both for ELMy H-mode baseline and for hybrid scenarios. Quite a number of successful high power experiments have been recently performed at JET in both scenarios with plasma density provided either with gas fuelling only or with combined low gas puff and pellet injection showing a neutron rate up to $2.8 \times 10^{16} \text{ sec}^{-1}$ [1,2]. The idea is to reproduce these DD pulses in DT plasmas, first keeping the auxiliary power at the original level of 33 MW, then increasing the power to the maximum JET availability (40 MW). Apart from a variety of problems related to the technical feasibility of such a challenge a non-marginal issue refers to the aim of keeping the maximum performances for 5 s, with the related long lasting power load to the divertor plates. In the above mentioned DD experiments the goal of sustainable plate power was reached by strike point sweeping, but the question arises if this technique might be sufficient for the DT plasmas, considering the additional contribution of the alpha- power and the planned longer flat top phase as well as the higher level of auxiliary power. Although power as well as Ne seeding scans (nitrogen seeding is not an option for the JET tritium handling facility) have already been simulated in view of the DT phase of JET on the basis of general discharge parameters [3] our study intends to contribute to understanding the operational constraints starting from selected high performance experimental JET pulses.

This paper is focused on the simulation of the power load on the divertor target of high performance JET-ILW ELMy H-mode DD pulses pertaining to the baseline scenario and to their numerical extension to the corresponding DT pulses. We have selected two pulses ($I_p = 3 \text{ MA}$, $B_t = 2.8 \text{ T}$) at medium density ($n_e = 6.5 - 7 \times 10^{19} \text{ m}^{-3}$) which show very high neutron rates and are characterized by $T_i/T_e > 1$ [1], with $T_e(0)$ about 7 KeV. The auxiliary power, P_{aux} , is in excess of 30 MW provided mostly by NBI, with ICRF heating level around 5 MW. For one of them (JPN 92436, record neutron flux, $H_{98}=1.1$) the density was provided by combined low level gas puff and pellet injection (hereafter: pellet) while for the other one (without pellets, $H_{98}=1$) the gas fuelling rate was at medium level, $1.8 \times 10^{22} \text{ e/s}$ (hereafter: gas puff). As a consequence, the SOL density in the pulse with gas fuelling only is higher than that in the pulse with pellets. A peculiar aspect of these pulses is their magnetic configuration with the outer strike point close to the pump out valve, the so-called corner configuration (see Fig. 1). This has some implications both for the experimental determination of the edge parameters of the pulses and for the modeling of the W penetration into the plasma.

These pulses are slightly Ne seeded (c_{Ne} about 0.1- 0.15 % in the core, from CXRS) and although the radiated power fraction, f_{rad} , is quite similar in the two pulses (about 0.40), the ratio of the radiated

power in the SOL to the total one ($P_{rad}^{SOL}/P_{rad}^{TOT}$) is = 0.15 for the pulse with pellets and it is = 0.21 for that with gas puffing, related to the different SOL densities.

The W atoms which enter the divertor plasma are only a small fraction of the sputtered ones (< 10%) due to prompt re-deposition processes. The geometry of the system for the corner configuration (Fig.1) with the outer strike point close to the pump out valve, is such that a fraction of the sputtered W atoms at the outer target is deposited directly onto non-accessible areas, thus not contributing to the W flux. Considering the slab geometry of the divertor in COREDIV (see Sect. 2), this is technically accounted for by reducing the W sputtering yield level, by about one third, with respect to the COREDIV setting used for other magnetic configurations. A second issue refers to the fact that for both these experimental pulses a significant amount of Ni is released by the interaction of the radiofrequency fields with the wall ($c_{Ni} = 4 \times 10^{-4}$ and 5.5×10^{-4} for the pulses with puffing and with pellets, respectively, see Fig.2).

Considering that, after numerical reconstruction of the experimental DD JET pulses, these pulses will be extrapolated to the DT plasmas with consequent production of He, we will be faced to five impurities: the intrinsic Be and W, and Ne, Ni and He. Although the number of impurity species which can be used in COREDIV is, in principle, not limited, we have considered in the present simulations only four impurities in order to limit CPU time required to achieving the steady state solution. Therefore, we had to choose either Ne or Ni for the simulation of the experimental DD pulses, since once the experimental pulses are numerically re-constructed, the simulation of the corresponding DT plasmas is performed by keeping everything unchanged, but only DT instead of DD. In fact, this study is limited to the evaluation of the thermal DT fusion reactions neglecting all possible other components of the fusion power as, for example, the beam-target component as well as the influence of supra-thermal ions generated in the specific ICRH scenario chosen. However, note that the contribution of the above mentioned neglected components of the alpha-power is marginal to the evaluation of the total power to the plate, which is the aim of the present study. Although most of the simulations have been performed with Ne, some tests in which Ne is replaced by Ni show substantial agreement. Indeed, both with Ne or with Ni all the experimental main parameters of the two pulses (as the core T_e , T_i and n_e profiles as well as the total stored energy and radiated power in the core and in the divertor and the core Z_{eff}) are satisfactorily reproduced in the simulations.

As a further step, P_{aux} is increased to 40 MW (assumed to be the maximum power level achievable in JET) and simulations of the two DT plasmas are performed either by keeping I_p , B_t , the H_{98} factor and n_e as at the original levels or by increasing the plasma current to $I_p = 4$ MA, and accordingly $B_t = 3.73$ T, and keeping unchanged the H_{98} factor as well as the Greenwald density fraction. At $P_{aux} = 40$ MW

for both pulses and both plasma currents the power load to the target plate increases at a non-sustainable level, with related need for additional neon seeding.

In Sect.2 the COREDIV model for the core and the SOL is shortly described. Sect. 3 is devoted to the experimental data and to the simulation of the two experimental DD pulses. The simulation of the corresponding DT pulses together with their extension to $P_{aux} = 40$ MW and the numerical neon seeding scan are discussed in Sect. 4. Conclusions are drawn in Sect. 5.

2 COREDIV MODEL

We have used the COREDIV code [4], self-consistent with respect to the core-SOL as well as to impurities-main plasma. In spite of some simplifications, especially in the SOL model (slab geometry and model of the neutrals), the exchange of information between the core (1D) and the SOL (2D) module renders this code quite useful when, as in the case of the JET-ILW, the interaction SOL-core is crucial.

In the core, given as code input the volume average electron density $\langle n_e \rangle$, the 1D radial transport equations for bulk ions, for each ionization state of impurity ions and for the electron and ion temperature are solved. The electron and ion energy fluxes are defined by the local transport model proposed in ref. [5] which reproduces a prescribed energy confinement law. In particular, the anomalous heat conductivity is given by the expression $\chi_{e,i} = C_{e,i} * a^2/\tau_E * F(r)$ where r is the radial coordinate, a is the plasma radius, τ_E is the energy confinement time defined by the ELMy H-mode scaling law and the coefficient ($C_e = C_i$) is adjusted to have agreement between calculated and experimental confinement times. The parabolic-like profile function $F(r)$, which may slightly change from run to run in order to match with the actual profiles of the experimental pulse to be modelled, can be modified at the plasma edge to provide for a transport barrier of chosen level. The main plasma ion density is given by the solution of the radial diffusion equation with diffusion coefficients $D_i = D_e = 0.2 \chi_e$, as in ref. [5]. Note, however, that the solution of the diffusion equation is largely independent of the exact value of D_e/χ_e . Indeed, a change in D_e/χ_e causes a consistent change in the source term, since the average electron density is a COREDIV input. For the auxiliary heating, parabolic-like deposition profile is assumed $P_{aux}(r) = P_0 (1-r^2/a^2)^y$ where y is in the range 1.5-3, depending on the quality of the auxiliary heating, NBI or/and ICRF. In conclusion: once the power deposition profile, the confinement time τ_E and the profile function $F(r)$ are assigned the electron temperature and density profiles are unambiguously determined. For the pulses considered in this study $y=2$. Impurity diffusion coefficient is set to be equal to that of the main ions and the anomalous impurity pinch, which is a code input, is set to zero for these two pulses (see Sect.3).

In the SOL we use the 2D boundary layer code EPIT, which is primarily based on Braginskii-like equations for the background plasma and on rate equations for each ionization state of each impurity species. An analytical description of the neutrals is used, based on a simple diffusive model. COREDIV takes into account the plasma (D and seeded impurities) recycling in the divertor as well as the sputtering processes at the target plates including deuterium and Be sputtering, self-sputtering and sputtering due to seeded impurities. (For deuterium and neon sputtering and tungsten self-sputtering the yields given in refs. [6,7] are used). The recycling coefficient is an external parameter which in COREDIV depends on the level of the electron density at the separatrix, n_{e_sep} , given as an input, and increases with increasing n_{e_sep} .

A simple slab geometry (poloidal and radial directions) with classical parallel transport and anomalous radial transport ($D_{SOL} = \chi_i = 0.5 \chi_e$, where χ_e ranges typically 0.4-1 m^2/s), is used and the impurity fluxes and radiation losses by impurity ions are calculated fully self-consistently. Although the values of the transport coefficients in the SOL are generally quite comparable to those at the separatrix, in the present simulations the value of D_{SOL} is set arbitrarily (in the range 0.2-0.3 m^2/s) in order to match with the core-SOL distribution of the radiated power (see Sect.3). All the equations are solved only from the mid-plane to the divertor plate, assuming inner-outer symmetry of the problem. This implies that the experimental in-out asymmetries, observed especially at high density-high radiation level, are not reproduced in COREDIV results. However, for all the different situations examined so far (with carbon plates and with the ILW, and with different seeding levels [8]) the COREDIV numerical reconstructed total radiation in the SOL matches well with the total experimentally measured SOL radiation, indicating that for JET conditions the edge-core COREDIV model can describe the global trend of this important quantity. The coupling between the core and the SOL is made by imposing continuity of energy and particle fluxes as well as of particle densities and temperatures at the separatrix. The computed fluxes from the core are used as boundary condition for the SOL plasma. In turn, the values of temperatures and of densities calculated in the SOL are used as boundary conditions for the core module.

3 EXPERIMENTS AND SIMULATION OF DD PLASMAS

Due to the corner magnetic configuration of the considered discharges, probe measurements are missing (no probe on, or near, the outer strike point) as well as many spectral line intensity measurements. The only available SOL data are the intensity of Be I line at 441 nm taken along a horizontal chord at the mid-plane, reflectometry measurements taken along a vertical line of sight in the upper far SOL and bolometric data. For the core plasma we refer to bolometry for the radiated power, to HRTS for T_e and n_e profiles, to SXR and VUV spectroscopy for heavy impurity radiation and concentration, to visible bremsstrahlung for Z_{eff} and to CXRS of seeded neon, intended for T_i measurement. Since the differential ratio of the radiated power to Z_{eff} ($\Delta P_{rad}/\Delta Z_{eff}$) is a factor 3-4

higher for W than for Ni in the relevant range of temperatures and charge stages in these pulses 8-9, the W sputtering yield had to be reduced and simultaneously the Ne puffing rate had to be increased above the experimental level in order to match both the experimental Z_{eff} and the core radiated power. One has to recall, indeed, that in our simulations, differently than in the experiments, Ni is not included and therefore the simulated core radiation is practically entirely due to W and Z_{eff} is practically entirely due to Ne. By successive adjustments, the reduction in the W sputtering yield by Ne came out to be 30-40 percent. With respect to impurity particle transport, the anomalous pinch velocity has been set to zero in these simulations (see Sect. 2), according to modeling of JET pulses [10], which show vanishing inward pinch velocity at high input power. Although the volume average density is similar for these pulses ($\langle n_e \rangle = 7.0$ and $6.6 \times 10^{19} \text{ m}^{-3}$ for the gas puff and the pellet pulse, respectively), as well as $P_{aux} = 33 \text{ MW}$, the density at the separatrix is set as 3.2 (gas puff) and $2.4 \times 10^{19} \text{ m}^{-3}$ (pellet) and $D_{SOL} = 0.25$ and $= 0.20 \text{ m}^2/\text{s}$, respectively, **in order to match the numerical results simultaneously both with reflectometry and bolometric data in the SOL. With these code inputs, the most relevant experimental and simulated quantities are summarized in Table I for the two pulses. The numerical results are compared with experimental data averaged over several ELM periods [11] since production as well as flushing out of W due to individual ELMs are not accounted for in the present steady-state COREDIV model.**

In the simulations, c_{Ne} , $P_{rad}^{SOL}/P_{rad}^{TOT}$ and c_W are significantly higher than in experiment. This is a consequence of the higher Ne seeding level used in the simulations to compensate for neglecting the Ni contribution to P_{rad} and Z_{eff} . With respect to the Be flux, considering that the level of the measured Be I line is about a factor of three higher in the pulse with gas puff and that the ionization per photon (S/XB) for the Be I line is rather insensitive to changes in electron temperature from about 3-4 eV to 100 eV (S/XB about 100, see ref. [12]), the level of the Be source in COREDIV has been set as $3.4 \times 10^{21} \text{ s}^{-1}$ and $1.18 \times 10^{21} \text{ s}^{-1}$, for the two pulses, respectively. To give an example, in Fig. 3 the experimental and reconstructed density and temperature core profiles for the pulse with pellets are compared.

4 SIMULATION OF DT PLASMAS

4.1. Simulation of DT plasmas at $I_p = 3 \text{ MA}$

Replacing DD by DT while keeping unchanged the auxiliary power level and the confinement enhancement factor H_{98} as well as the Ne seeding rate doesn't lead in our simulations to major differences both for the pulse with pellets and for that with gas puff what the target power load is concerned. (Please, recall that our simulations are limited to the estimation of the thermal component of the α -power). The slight increase in τ_E (mass dependence) together with the little contribution of P_α (0.5 MW and 0.7 MW for the two pulses, respectively) lead in COREDIV only to a little increase

in the power to the plate. At $P_{aux}=40$ MW the situation changes in relation to the power to the target. Indeed, the little increase in c_w and in the core radiation is not sufficient to compensate for the higher input power, resulting in a significant increase in the power to the SOL and to the target, see Table 2.

The target power load can be mitigated by increasing the level of Ne seeding which leads to different scaling depending on which parameter is kept as constant in the simulations: the H_{98} factor (total energy) or the energy (and particle) transport coefficients. Indeed, depending on the specific JET-ILW experimental situation, in some cases the H_{98} factor decreases [13] with increasing the Ne seeding level, in others it remains nearly constant [14] and in some others it may increase [15]. We have chosen to perform a Ne seeding scan for the two considered pulses keeping constant the H_{98} factor. Note that, without excluding possible SOL modifications, in the case the total plasma energy is set to remain constant with increasing the Ne seeding rate the *net energy confinement time*, $W/(P_{in}-P_{rad}^{CORE})$, and the *effective* τ_p (effective particle residence time) increase during the Ne seeding scan since the power lost into radiation in the plasma core generally increases too. This leads to a further enhancement in the core radiation, which, on the other hand, tends to limit (self-consistently) the tungsten sputtering. In Fig. 4 the main code outputs for the Ne seeding scan at $I_p=3$ MW with $P_{aux}=40$ MW are shown for the two pulses.

In both Ne scans the power to the plate can be reduced to less than 13 MW with some differences, however, for the two pulses. For the pulse with pellets, although the power to the SOL is lower than that for the gas puff one, T_E^{PLATE} is higher and saturates at about 18 eV, due to the lower SOL density. This is correlated with the low P_{rad}^{SOL} and the high c_w . With respect to the α -power, COREDIV simulations predict an increase in the thermal P_α level at higher Ne seeding rate as a consequence of the increase in the main ion temperature, dependent on the main ion dilution [14]. Decreasing the power to the plate with Ne seeding from 22MW to 15 MW, P_α increases from 0.59 to 0.66 MW for the pulse with gas puff and from 0.85 to 0.96 MW for that with pellets. If, on the other hand, one assumes the constancy of the fusion reactivity (at the level of the lowest Ne seeding rate), the α -power decreases with increasing the neon seeding rate, from 0.59 to 0.45 MW and from 0.85 to 0.68 MW, respectively, see Fig. 5. Indeed, in this case only the increase in fuel dilution counts.

4.2. Simulation of DT plasmas at $I_p = 4$ MA

Another possible scenario for JET-ILW DT experiments consists in performing the two above discussed pulses keeping $P_{aux}=40$ MW, but at higher plasma current $I_p = 4$ MA and, consistently, $B_t = 3.73$ T ($q_{95}=3$). COREDIV simulations for this scenario have been performed keeping unchanged the original experimental confinement factors ($H_{98} = 1.0$ and 1.1 , for the gas puff and pellet pulses, respectively) as well as the density Greenwald fractions ($f_{Gw}=0.65$ and 0.63 , respectively) and

keeping unchanged also the ratio of the density at the separatrix to the average one. As a starting point, the Ne seeding rate for the two DT pulses with $P_{aux} = 40$ MW at $I_p = 4$ MA has been kept at the same level of the simulations of the original DD pulses (see Sect. 3).

The combined effect of higher τ_E and higher electron density leads at $I_p = 4$ MA to a significant increase in the thermal α -power ($P_\alpha = 1.58$ MW and 2.22 MW for the gas puff and the pellet, respectively) with nearly unchanged power load to the target, as compared to the simulations at $I_p = 3$ MA (see Figs. 6 and 7). The little increase in the SOL radiation is accompanied with the reduction in the temperature at the plate and with the decrease in W sputtering and therefore in W core concentration. As a consequence of the high electron density, and therefore of the low Ne concentration, Z_{eff} is rather low ($= 1.42$ and 1.56 for the gas puff and pellet, respectively). In order to mitigate the target power load, which is $P^{PLATE} = 21.51$ MW and 21.24 MW for the gas puff and pellet pulses respectively, a Ne seeding scan has been numerically performed resulting in the possibility of decreasing P^{PLATE} below 15 MW at Z_{eff} below 2.3 for both pulses, see Fig. 6. The main differences between the two sets of Ne seeding simulations at $I_p = 4$ MA is seen, as in the case at $I_p = 3$ MA, in the ratio of $P_{rad}^{SOL} / P_{rad}^{TOT}$ which is significantly higher in the gas puff pulse, and in T_e^{PLATE} which is lower by 3-4 eV in the gas puff pulse. With respect to the change in P_α with increasing the Ne seeding rate, in Fig. 7 two curves are plotted for each pulse (as it was done in the case of $I_p = 3$ MA), one refers to the assumption of self-consistent COREDIV reactivity (T_i increases with Ne seeding level), the other to the assumption of constant reactivity. As in the case of $I_p = 3$ MA, with increasing Ne seeding P_α increases by about 10 percent with self-consistent reactivity and it decreases slightly at constant reactivity.

5 SUMMARY AND CONCLUSION

Two similar **JET-ILW** high performance pulses, one with gas puff only and another with combined low gas + pellet fuelling, have been numerically simulated resulting in a target load of 16-17 MW. While the two pulses are similar in input power (about 33 MW) as well as in radiated power (13-14 MW), their main difference, as far as the here reported simulations are concerned, refers to the edge density, which in the pulse with pellets is lower than in the one with gas fuelling only, resulting in slightly higher plate temperature: 19 eV for the pellet pulse and 17.5 eV for the gas puff one. Since for the two experimental pulses a significant amount of Ni is detected (especially for that with pellets) the W sputtering yield had to be reduced and an amount of Ne larger than in experiment had to be seeded in order to numerically reproduce the total radiated power and Z_{eff} . Indeed, in the COREDIV simulations here presented the number of impurities is limited to four. Extrapolation to DT plasmas, keeping unchanged input power, leads to little difference with respect to the reconstructed DD pulses, with thermal alpha-power (the only component of P_α we are concerned with) of about 0.5 MW and 0.7 MW for the pulse with gas puff only and with pellets, respectively. The most relevant result of the

extrapolation of the DD pulses to DT plasmas at $P_{aux}=40$ MW at the original $I_p=3$ MA shows, together with the little increase in thermal P_α (0.59 MW and 0.85 MW for the gas puff and pellet, respectively), the enhancement of the power to the target, which becomes in excess of 21 MW in the simulations, for both pulses. At $P_{aux} = 40$ MW and $I_p = 4$ MA, due to the higher τ_E and electron density, the thermal P_α reaches 1.58 MW (gas puff) and 2.22 MW (pellet), but the power to the target remains at about 21 MW, as in the simulations at $I_p = 3$ MA, although T_e^{PLATE} is slightly reduced. In fact, for both scenarios the relatively small increase in the radiated power is not sufficient to compensate for the increase in the input power. In order to investigate for a possible mitigation of the power to the plate a numerical Ne scan has been performed, showing the possibility of achieving P^{PLATE} below 15 MW in both scenarios with $Z_{eff}=2.6$ (gas puff) and $Z_{eff}= 3.0$ (pellet) at $I_p = 3$ MA, and $Z_{eff}=2.3$ (gas puff) and $Z_{eff}= 2.2$ (pellet) at $I_p = 4$ MA. At $P^{PLATE} = 15$ MW, P_α may increase or decrease by about 10 percent with respect to the un-seeded case, depending on the assumption made for the fusion reactivity.

Recalling that the numerical results for the DT plasmas here presented refer only to the thermal alpha-power (the total P_α is expected to be higher by a factor 1.5 – 2.0) and considering the number of assumptions made for the reconstruction of the experimental pulses as well as for the Ne seeding scan of the DT plasmas at $P_{aux}= 40$ MW, only qualitative conclusions can be drawn from this study. However, even though the pulse with combined low gas puff and pellet injection shows significantly higher performance in the DD experiments as well as in the DT simulations, this pulse requires higher tungsten concentration (or, in general, higher P_{rad}^{CORE}) to reduce P^{PLATE} to sustainable levels for 5s steady-state operation, due to the reduced SOL density and related reduced SOL radiation. This may render the control of the power to the plate more critical for the pulse with pellets than for the pulse with gas puff only.

From the experimental point of view, amongst other mechanisms affecting the target heat load not included in the simulations here presented are the increase of the strike-point sweep amplitude (planned for next coming experiments) and the potentially expected increase in the core plasma density (better particle confinement) when extrapolating from DD to DT [16], which can both relieve somewhat the levels of seeding needed for divertor heat load control.

ACKNOWLEDGEMENTS

The authors are grateful to M. O' Mullane for his kind help with providing the ADAS data. This work has been carried out within the framework of the EUROfusion Consortium and has received funding from the Euratom research and training programme 2014-2018 under grant agreement No 633053. The views and opinions expressed herein do not necessarily reflect those of the European Commission. This scientific work was financed within the Polish framework of the scientific financial resources in 2018 allocated for realization of the international co-financed project.

REFERENCES

- [1] H.T. Kim et al. Nucl. Fusion, **58** (2017) 036020
- [2] J. Hobirk et al. Plasma Phys Control Fusion (2012) **54** 095001
- [3] R. Zagorski et al. Contributions to Plasma Physics, **6** December 2017
- [4] R. Zagorski, et al., Nucl. Fusion **53** (2013) 073030
- [5] J. Mandrekas and W.M. Stacey, Nucl. Fusion **35** (1995) 843
- [6] Y. Yamamura, et al., Report of the IPP Nagoya, IPPJ-AM-26 (1083)
- [7] C. Garcia-Rosales et al., J. Nuclear. Mater. 218 (1994) 8-17
- [8] T. Putterich et al., " Tungsten Screening and Impurity Control in JET 2012 Proc. 24rd IAEA Fusion Energy Conf., San Diego, CA 8-13 October 2012 (Vienna: IAEA) vol. IAEA-CN-197, EX-P3.1
- [9] A. Czarnecka et al., Plasma Phys. Control. Fusion (2011) **53** 035009
- [10] M. Valisa, et al., 44th EPS Conf., Belfast 2017
<http://ocs.ciemat.es/EPS2017ABS/pdf/P4.174.pdf>
- [11] G. Telesca et al. J. Nucl. Mater. doi:10.1016/j.jnucmat.2014.11.024
- [12] [http://open.adas.ac.uk/detail/adf13/sxb96\[\[be/sxb96\]\]\[\[be_pju\]\]\[\[be0.dat](http://open.adas.ac.uk/detail/adf13/sxb96[[be/sxb96]][[be_pju]][[be0.dat)
- [13] C. Giroud et al. "Towards baseline operation integrating ITER-relevant core and edge plasma within the constraint of the ITER-like wall at JET" 45th EPS Conference, Prague 2018, Paper EX/P5-25
- [14] S. Gloeggler et al. "Study of the Impact of High Neon Radiation on Pedestal and Divertor in JET Experiments" 45th EPS Conference, Prague 2018, Paper EX/P2.1025, to be submitted to Nuclear Fusion
- [15] G. Telesca et al., Nucl. Fusion (2017) **57** 126021
- [16] C. Maggi et al., Plasma Phys. Control. Fusion (2018) **60** 014045

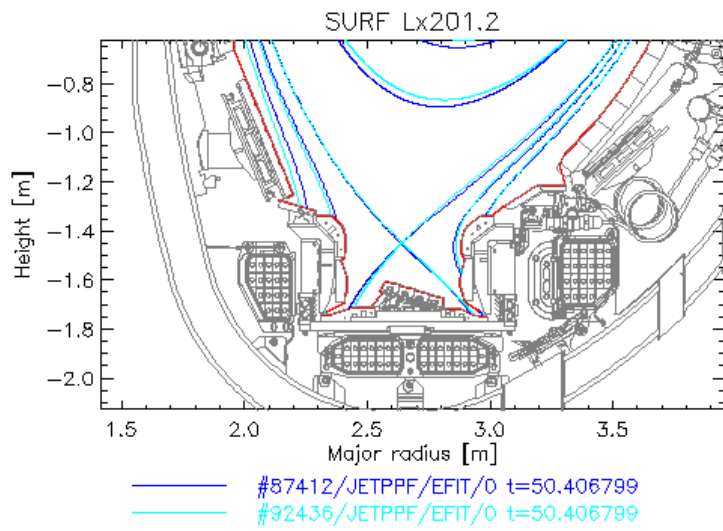


FIG. 1. Corner magnetic configuration

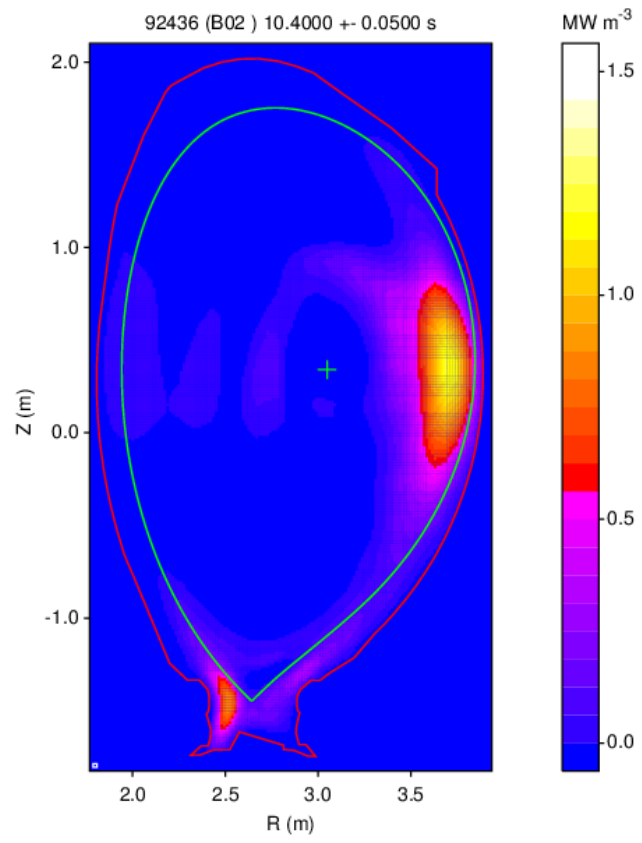


FIG.2. Tomographic reconstruction of the radiated power density of JPN 92436 $t= 10.4$ s. The highest radiation density at the mid-plane in the LFS is due to N

TABLE 1. $P_{TOT} = 33$ MW, SUMMARY OF EXPERIMENTAL AND SIMULATED QUANTITIES

PARAMETERS	# 92432 , $t = 9.5s$		# 92436 , $t = 10.4s$	
	Exp	Sim	Exp	Sim
W_{th} [MJ]	8.1	8.0	8.7	8.9
P_{rad}^{TOTAL} [MW]	13.9	13.8	13.5	13.8
$P_{rad}^{SOL}/P_{rad}^{TOTAL}$	0.21	0.26	0.15	0.21
Z_{EFF}	1.55	1.55	1.7	1.71
P^{PLATE} [MW]	19*	16.85	19.5*	16.7
C_W [$\times 10^{-5}$]	1.5 ÷ 5	9.7	3.8 ÷ 4.9	12.1

*power to the plate in experiment: $P^{PLATE} = P_{TOT} - P_{rad}^{TOTAL}$

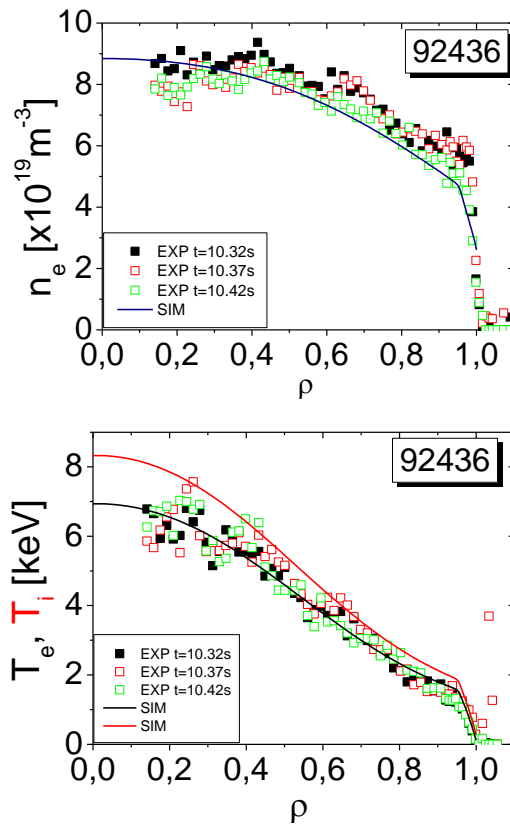


FIG. 3 . Experimental and simulated electron density and electron (and ion) temperature profiles for JPN 92436 $t= 10.4$

TABLE 2. PREDICTIVE SIMULATIONS FOR DT PLASMAS AT $P_{aux} = 40$ MW AND $I_p = 3$ MA

PARAMETERS	Gas puff	Pellet injection
	D-T, 40MW	D-T, 40MW
P_α therm.[MW]	0.593	0.846
W_{th} [MJ]	8.88	9.96
P_{rad}^{TOTAL} [MW]	16	15.36
$P_{rad}^{SOL}/P_{rad}^{TOTAL}$	0.25	0.22
Z_{EFF}	1.58	1.76
P^{PLATE} [MW]	21.3	21.3
C_W [$\times 10^{-5}$]	12.5	14.9
C_{Ne} [$\times 10^{-2}$]	0.18	0.46
T_e^{PLATE} [eV]	17.9	20.6

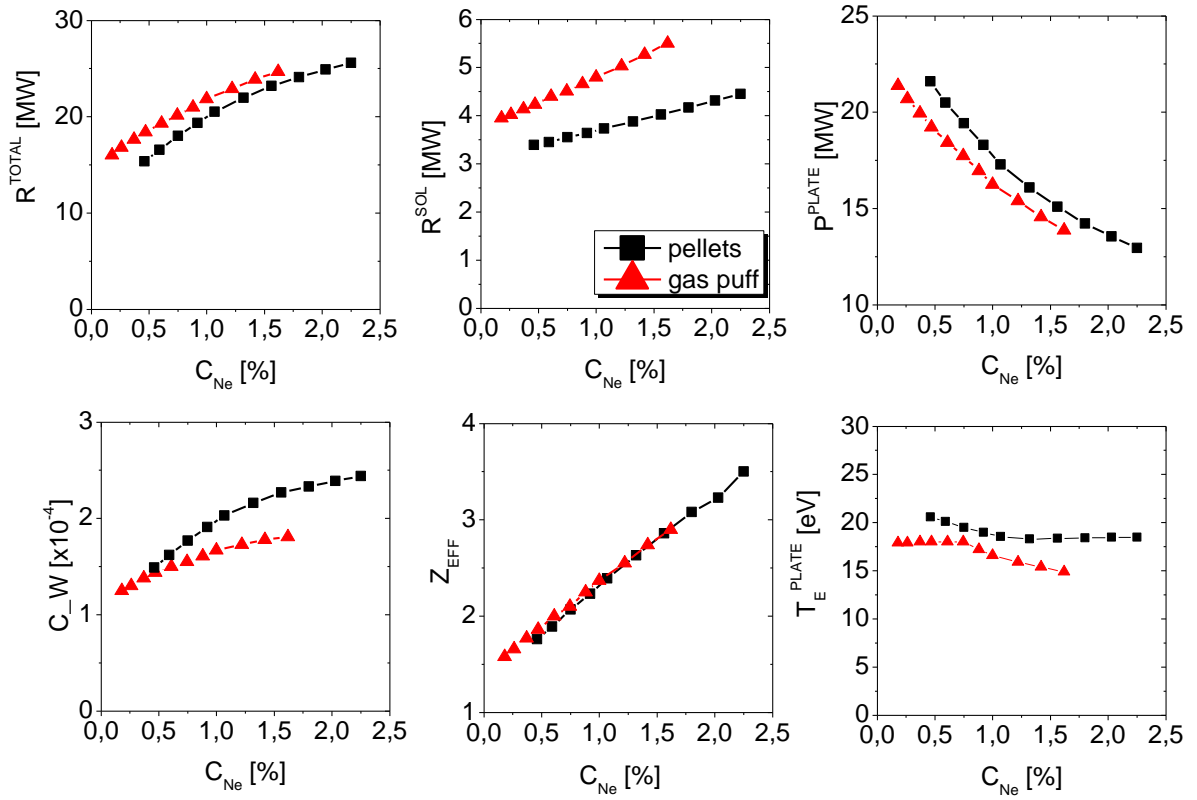


FIG. 4. Main COREDIV code outputs for Ne seeding scan in DT plasmas at $I_p = 3$ MA and $P_{aux} = 40$ MW at constant H_{98} factor as a function of Ne concentration. R^{TOTAL} = Total radiated power, R^{SOL} = Radiated power in the SOL, P^{PLATE} = Power to the target, C_W = W concentration, T_E^{PLATE} = electron temperature at the plate.

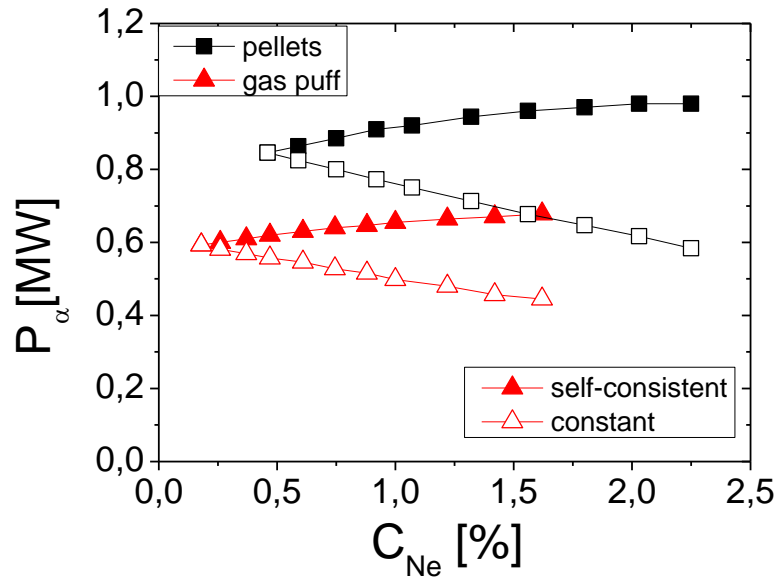


FIG. 5. Thermal alpha-power for the two pulses as a function of C_{Ne} for the case $I_p = 3$ MA and $P_{aux} = 40$ MW. The two curves for each pulse refer to the COREDIV self-consistent reactivity (full symbols) and to the reactivity kept constant at the level of the lowest Ne seeding rate.

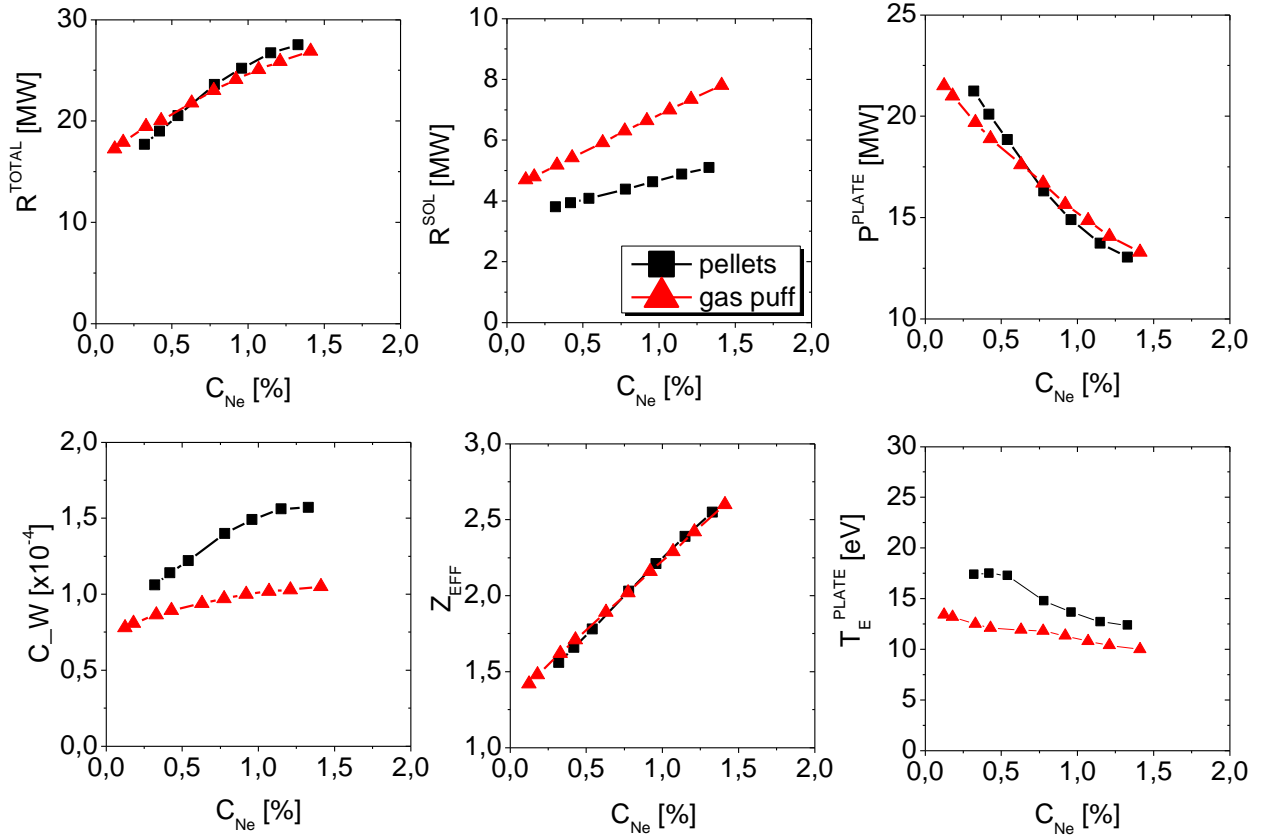


FIG. 6. Main COREDIV code outputs for Ne seeding scan in DT plasmas at $I_p = 4$ MA and $P_{aux}=40$ MW at constant H_{98} factor as a function of Ne concentration. R^{TOTAL} = Total radiated power, R^{SOL} = Radiated power in the SOL, P^{PLATE} = Power to the target, C_W = W concentration, T_E^{PLATE} = electron temperature at the plate.

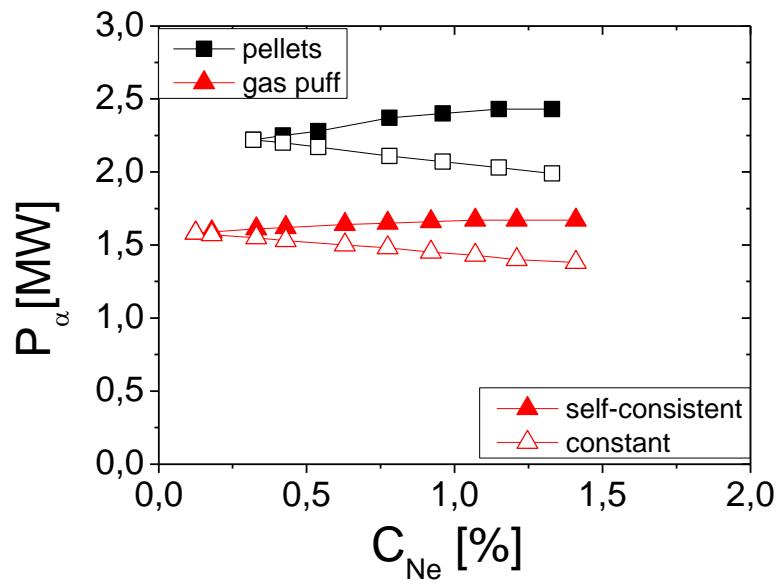


FIG. 7. Thermal alpha-power for the two pulses as a function of C_{Ne} for the case $I_p = 4$ MA and $P_{aux} = 40$ MW. The two curves for each pulse refer to the COREDIV self-consistent reactivity (full symbols) and to the reactivity kept constant at the level of the lowest Ne seeding rate